university of groningen

University Medical Center Groningen

University of Groningen

Anomalous Carrier Transport in Ambipolar Field-Effect Transistor of Large Diameter Single-Walled Carbon Nanotube Network

Bisri, Satria Zulkarnaen; Derenskyi, Vladimir; Gomulya, Widianta; Salazar-Rios, Jorge Mario; Fritsch, Martin; Froehlich, Nils; Jung, Stefan; Allard, Sybille; Scherf, Ullrich; Loi, Maria Antonietta

Published in:
Advanced electronic materials

DOI:
10.1002/aelm.201500222

IMPORTANT NOTE: You are advised to consult the publisher's version (publisher's PDF) if you wish to cite from it. Please check the document version below.

Document Version
Publisher's PDF, also known as Version of record

Publication date:
2016

Link to publication in University of Groningen/UMCG research database

Citation for published version (APA):
Bisri, S. Z., Derenskyi, V., Gomulya, W., Salazar-Rios, J. M., Fritsch, M., Froehlich, N., Jung, S., Allard, S., Scherf, U., & Loi, M. A. (2016). Anomalous Carrier Transport in Ambipolar Field-Effect Transistor of Large Diameter Single-Walled Carbon Nanotube Network. *Advanced electronic materials*, *2*, Article 1500222. https://doi.org/10.1002/aelm.201500222

Copyright
Other than for strictly personal use, it is not permitted to download or to forward/distribute the text or part of it without the consent of the author(s) and/or copyright holder(s), unless the work is under an open content license (like Creative Commons).

The publication may also be distributed here under the terms of Article 25fa of the Dutch Copyright Act, indicated by the “Taverne” license. More information can be found on the University of Groningen website: https://www.rug.nl/library/open-access/self-archiving-pure/taverne-amendment.

Take-down policy
If you believe that this document breaches copyright please contact us providing details, and we will remove access to the work immediately and investigate your claim.

Anomalous Carrier Transport in Ambipolar Field-Effect Transistor of Large Diameter Single-Walled Carbon Nanotube Network

Satria Zulkarnaen Bisri, Vladimir Derenskyi, Widianta Gomulya, Jorge Mario Salazar-Rios, Martin Fritsch, Nils Fröhlich, Stefan Jung, Sybille Allard, Ullrich Scherf, and Maria Antonietta Loi**

Single-walled carbon nanotubes (SWNTs) remain at the forefront of the most prospective materials for electronic device applications "beyond Moore's," despite the emergence of many other competing materials that include its own allotrope (graphene), and others graphene-like semiconductors. Not only do semiconducting SWNTs (sSWNTs) have a true bandgap that allow field-effect transistors to be completely turned off, but their 1D nature appears as the most suitable structure to support the current advancement goals in post-silicon electronics, such as nanometer dimensions (ultrathin body) allowing for high device density.[1] Moreover, carbon nanotubes offer the possibility of gating them all-around.[2] In complementary metal-oxide-semiconductor (CMOS) electronics, the high carrier mobility of the field effect transistor (FET) can contribute to lower dynamic power consumption. Furthermore, higher on/off ratio and steep subthreshold swing can contribute to lowering the static power necessary to the device.[3] It is therefore clear that SWNT FETs have great prerequisite for the development of post-silicon low-power consumption electronics. One of the main bottlenecks toward achieving this great potential is the coexistence of semiconducting and metallic SWNTs in as-synthesized samples.[4]

Over the past ten years, efforts to separate and purify semiconducting species of SWNTs have shown tremendous advancements.[5–9] Both covalent and noncovalent functionalization of SWNT walls demonstrated capabilities to select and individualize sSWNTs based on diameter and/or chirality with purity above 99%.[5,10]

One of the most intriguing and effective methods is the polymer-wrapping technique.[5,11] This technique relies on the capability of conjugated polymers to interact through van der Waals forces with the walls of sSWNTs of specific chirality. Different types of polymer backbones have been utilized, and one of the most effectives is the polyfluorene backbone. High performing ambipolar FETs with high mobilities for both charge carriers and high on/off ratio values ($\approx 10^7$) have been reported using networks of SWNTs purified through this method.[12] Furthermore, the modification of the polymer backbone using longer alkyl chains has been demonstrated effective to select different kinds of nanotubes with diameters up to 1.5 nm.[13] In the early studies of charge carrier transport of single strand SWNTs, it was predicted that large diameter SWNTs will provide better charge carrier transport due to lower carrier scattering from phonons.[14,15]

Recently, current modulation as high as 10^8 has been demonstrated in ambipolar FET made with semialigned networks of polymer-sorted SWNTs, reaching the value that is required for practical applications of these devices.[16] Despite the great progress that has been made in reproducible fabrication of sSWNTs-based FETs, to date, the nature of the charge carrier transport in nanotube networks are still rarely being discussed. The reported low mobility in most nanotube networks (<10 cm^2 V^{-1} s^{-1}),[12,16] in comparison with the one that can be attained by individual SWNTs ($\approx 10^5$ cm^2 V^{-1} s^{-1}),[17,18] makes researchers believe that charge transport in this system is limited by the network arrangement and by other components fractions (polymers, surfactants, impurities, and other moieties) which are present in the network, instead of being the property of the individual tubes. These factors undermine the prospects for utilization of SWNTs in both high performance electronic devices as well as in niche applications as flexible electronics.

Different authors have attempted to explain the transport mechanism in the network. Some reports proposed that the transport in SWNT networks, prepared by covalent functionalization, obeys the variable-range hopping (VRH) model with dimensionality that depends on the fraction of metallic tube species present in the network,[19] or alternatively, the length of the carbon nanotubes.[20] Other authors include the possibility of Tomonaga–Luttinger liquid behavior,[21] which arise from the 1D nature of the transport. Recently, Gao and Loo proposed that the charge carrier transport behavior in sSWNT networks is thermally activated, but it is non-Arrhenius and can be better fitted using a fluctuation-induced tunneling (FIT) model.[22] While this proposal is very intriguing, the experiments were conducted using unipolar (p-type) FETs made with a network

Dr. S. Z. Bisri, V. Derenskyi, W. Gomulya, J. M. Salazar-Rios, Prof. M. A. Loi
Zernike Institute for Advanced Materials
University of Groningen
Nijenborgh 4, Groningen 9747AG, The Netherlands
E-mail: satria.bisri@riken.jp; m.a.loi@rug.nl
Dr. S. Z. Bisri
RIKEN Center for Emergent Matter Science
2-1 Hirosawa, Wako, Saitama 351-0198, Japan
M. Fritsch, Dr. N. Fröhlich, Dr. S. Jung, Dr. S. Allard, Prof. U. Scherf
Chemistry Department and Institute for Polymer Technology
Wuppertal University
Gauss-Str. 20, Wuppertal D-42119, Germany

DOI: 10.1002/aelm.201500222

© 2015 WILEY-VCH Verlag GmbH & Co. KGaA, Weinheim

of sSWNT wrapped by poly[(9,9-dioctylfluorenyl-2,7-diyl)-alt-co-(6,6′-{2,2′-bipyridine})] block copolymer (PFO-BPy) that demonstrated modest mobility and on/off ratio. Therefore, these experiments give only a partial view of the SWNT network transport. Carbon nanotubes are intrinsic semiconductors and therefore ambipolar. However, several factors in the sample preparation and measurements can suppress the transport of electrons preventing gaining a complete picture of the charge carrier transport. Only with a well-controlled device fabrication process and measurement protocol,[12,16] ambipolar FETs of SWNTs with high carrier mobility and on/off ratio can be obtained.

Here, we report a study of the carrier transport mechanism in ambipolar FETs of semialigned networks of polymer-wrapped carbon nanotubes. The demonstration of ambipolar FETs with high on/off ratio provides the opportunity to investigate the transport mechanism of both electron and holes in sSWNTs.[23] The ambipolar characteristics persist with much improved on/off ratio values (10^6) when the FET is cooled down to liquid N_2 temperature. We observe that the mobility values of both holes and electrons decrease by cooling, but with some anomalies as a slight increase below 150 K. By scrutinizing the gate voltage dependent transport of both holes and electrons, we conclude that the increase of the charge carrier mobility is not due to any residual of metallic carbon nanotube species. The origin of the observed anomalous temperature-dependent carrier transport is due to the transition from a transport regime dominated by intertube interactions, which are influenced by the wrapping polymer, to a regime dominated by the intratube carrier transport that is determined by the 1D transport properties of the SWNTs.

Single-walled carbon nanotubes network FETs were fabricated on 230 nm thick SiO_2 dielectric with Au interdigitated bottom contact electrodes (**Figure 1**a). The whole device fabrication was performed inside a N_2 glovebox. Large diameter arc-discharge-synthesized (SO) semiconducting nanotubes were deposited from toluene-based solution onto the transistor channel using the blade coating technique to obtain a semialigned sSWNT network (see atomic force micrograph in Figure 1b). These large diameter nanotubes were selectively dispersed using the polymer-assisted separation method with poly(9,9-di-n-dodecylfluorenyl-2,7-diyl) (PF12) to obtain highly pure semiconducting nanotube solution.[13] The nanotube solution was enriched to remove the residual polymer chains, so that only those chains wrapped around the sSWNT remain.[12] The absorbance spectra of the sSWNT solution after separation and after the subsequent enrichment are shown in Figure 1c.

The FETs were measured in a cryostat probe station with liquid N_2 cooling. Subsequent to their insertion into the cryostat, the samples were annealed at 105 °C for 24 h in ultrahigh vacuum to remove any possible adsorption of oxygen or moisture occurred during sample transfer.

The I_D–V_D output characteristics of the FET measured at room temperature (300 K) and at 77 K are compared in Figure 1d. The device demonstrates ambipolar transport behavior. At room temperature, clear saturation regimes were observed for both holes and electron accumulations at $V_G = \pm 10$ V. At higher V_G values, the I_D–V_D trends of both holes and electrons enhancements approached their respective

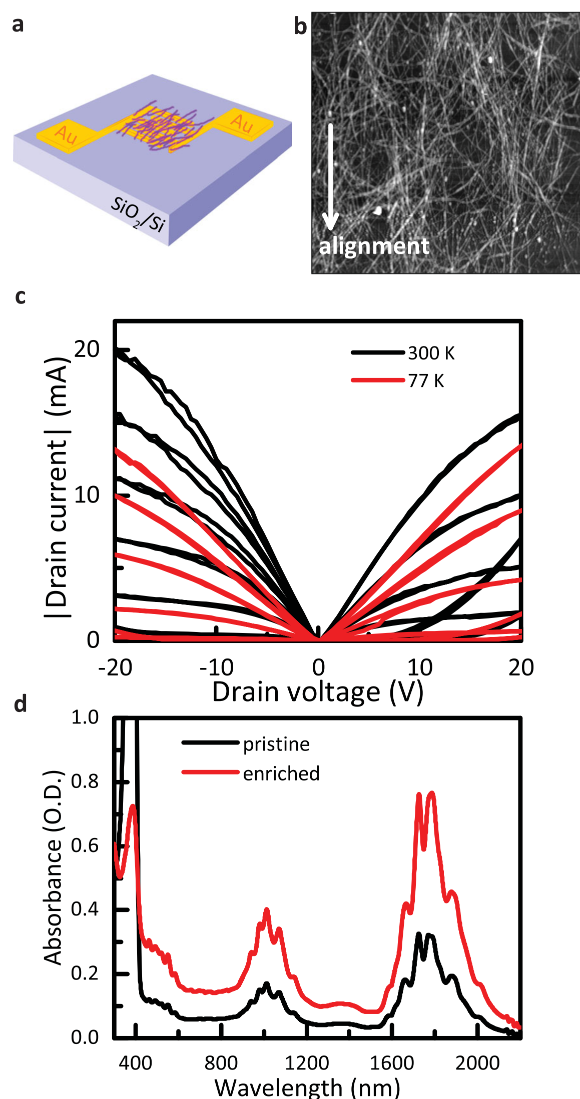

Figure 1. a) Structure of the field-effect transistor using semialigned polymer-wrapped single-walled carbon nanotubes (SWNTs). b) Atomic force microscopy (AFM) image of the semialigned SWNTs network deposited on the device structure. The image scan area is 8 µm × 8 µm. c) Absorption spectra of PF12-wrapped SO-nanotubes before (black line) and after (red line) enrichment. d) Comparison of I_D–V_D output characteristics of the ambipolar FET (L = 20 µm; W = 10 mm) measured at room temperature (red line) and at 77 K (blue line). The left part ($-20\,V < V_D < 0\,V$) shows the hole accumulation by increasing gate voltage from 0 to −50 V with 10 V increment; the right part ($0\,V < V_D < 20\,V$) shows the electron accumulation by increasing gate voltage from 0 to 50 V with 10 V increment.

pinch-off points. At 77 K, the device still shows ambipolar transport with distinguishable linear and saturation regimes for both holes and electrons, in particular at low V_G values. At low drain voltage value ($V_D < 5$ V), the linearity of the I_D demonstrates the nearly Ohmic injection of both holes and electrons, which remains unchanged by decreasing the temperature. The contact resistance values for both holes and electron injections at room temperature and low temperature condition were extracted using the Y-function method.[24] The increase of

 © 2015 WILEY-VCH Verlag GmbH & Co. KGaA, Weinheim

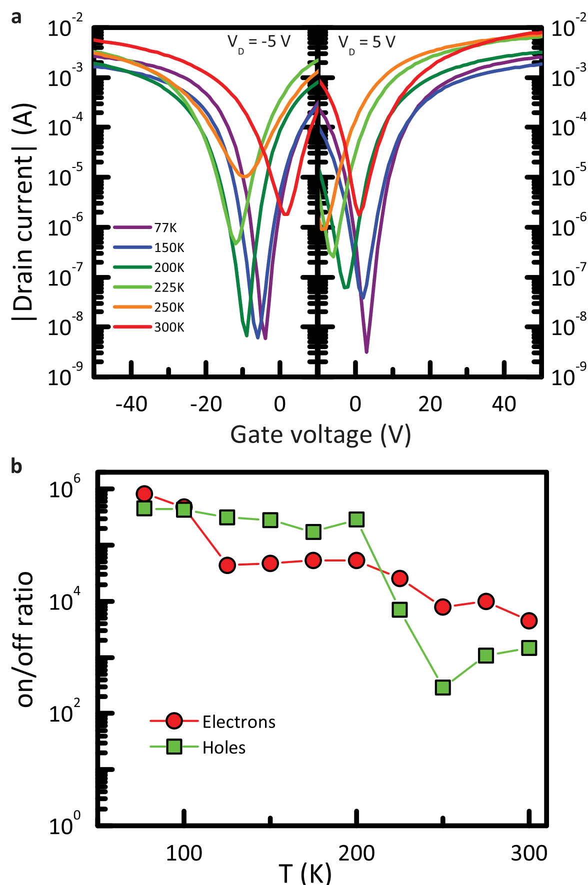

Figure 2. a) Temperature dependent evolution of the p- and n-channel I_D–V_G transfer characteristics of the ambipolar FET. b) The temperature dependence of the current modulation ratio (on/off ratio) of the FET for both hole and electron enhancement regimes.

contact resistance by decreasing the temperature is lower than a factor of two. At 300 K, the contact resistance of holes and electrons are 114.50 Ω mm and 34.19 Ω mm, respectively. At 77 K, the values became 269.80 Ω mm for holes injection and 96.35 Ω mm for electrons injection. The maxima of the contact resistance values are 148.94 Ω mm (at 125 K) and 447.04 Ω mm (at 150 K), for electrons and holes, respectively. The obtained contact resistance values are relatively low, indicating only a small influence from the mismatch between the Fermi level of the Au metal electrodes and both valence and conduction bands of the large diameter sSWNTs. This also indicates that the presence of the polymer wrapping does not seriously affect the charge carrier injection. The extracted contact resistance values are used to obtain the intrinsic (contact-resistance-free) channel mobility values.

In the displayed I_D–V_G transfer characteristics (**Figure 2**a), the room temperature on/off ratio values for hole and electron accumulation in this large diameter SWNT FETs is in the order of 10^4. This value confirmed the results obtained in ambipolar FET of similar polymer-wrapped large diameter SWNT gated using ionic liquid based gel.[13] However, this on/off is lower than the state-of-the-art SWNT network FET, which was demonstrated using semialigned small diameter HiPCO nanotube wrapped by P3DDT polymer that exhibited less pronounced ambipolar transport and more holes dominated characteristics.[16]

Cooling down the ambipolar FET to 77 K only a slight decrease of the on-current for both holes and electron is observed. On the other hand, the off-current values decrease at low temperature of more than 2 orders of magnitudes. At 77 K, the on/off ratio of the ambipolar FET reaches 10^6 for both holes and electron accumulations (Figure 2b). The off-current can originate either from carrier trap states or from mobile charged impurities.[25,26] The increase of the on/off ratio, predominantly caused by the decrease of the off-current, by lowering the temperature indicates that the trap states become inaccessible from either the valence and the conduction bands. Furthermore, the mobile charge impurities (if any) would not be able to contribute to charge carrier transport at low temperature. The high on/off ratio through off-current lowering also confirms that the SWNT network does not contain metallic species. If the source of the high off-current at room temperature would have been the large number of metallic SWNTs, the current would not decrease at low temperature. It is also important to underline that all measured FETs have a relative short channel length (20 µm) and that the on/off ratio of 10^6 is the highest ever reported for ambipolar FET using large diameter (>1.2 nm) sSWNTs.

The effective mobility values of holes and electrons were extracted from the simplified Y-function of the I_D–V_G transfer characteristics in the linear regime ($V_D \ll V_G$). A simplified Y-function can be expressed as[24]

$$Y = \frac{I_D}{\sqrt{g_m}} = \sqrt{\mu_o C_{ox} V_D \frac{W_C}{L_C}} (V_G - V_{Th}) \quad (1)$$

where L_C and W_C are the channel length (L_C = 20 µm) and width (W_C = 1 cm), respectively, and g_m is the transconductance (dI_D/dV_G). We use the parallel plate model for the capacitance where $C_{ox} = \varepsilon\varepsilon_0 / t_{ox} \approx 15\text{nF cm}^{-2}$ with ε is the dielectric constant and t_{ox} is the thickness of the SiO_2, since the density of the carbon nanotubes on the channel is well above the percolation limit.[12,16] Moreover, the network of SWNTs is only partially aligned. **Figure 3**a shows the temperature dependent mobility values for both holes and electrons of the sSWNT FET extracted from the transfer characteristics at $|V_D|$ = 5 V (linear regime). In comparison with standard FET mobility deduction,[27] the usage of Y-function allows us to obtain the mobility values which are free from the influence of contact resistance.[24] At room temperature, the mobility values for holes and electrons are as high as 5.68 cm^2 V^{-1} s^{-1} and 10.39 cm^2 V^{-1} s^{-1}, respectively. Between 300 K and 175 K, both hole and electron mobility monotonously decreases with decreasing temperature. At 150 K, the electron mobility became 2.16 cm^2 V^{-1} s^{-1}. On the other hand, the minima of the hole mobility occurred at 200 K with a value of 2.14 cm^2 V^{-1} s^{-1}. The decrease of the charge carrier mobility values of both holes and electrons is consistent with an Arrhenius-like trend. However, below 150 K, the mobility values deviate from these linear trends. Both hole and electron mobility increase anomalously when the temperature is further lowered below 125 K down to 77 K reaching 3.96 cm^2 V^{-1} s^{-1} and 3.29 cm^2 V^{-1} s^{-1},

© 2015 WILEY-VCH Verlag GmbH & Co. KGaA, Weinheim

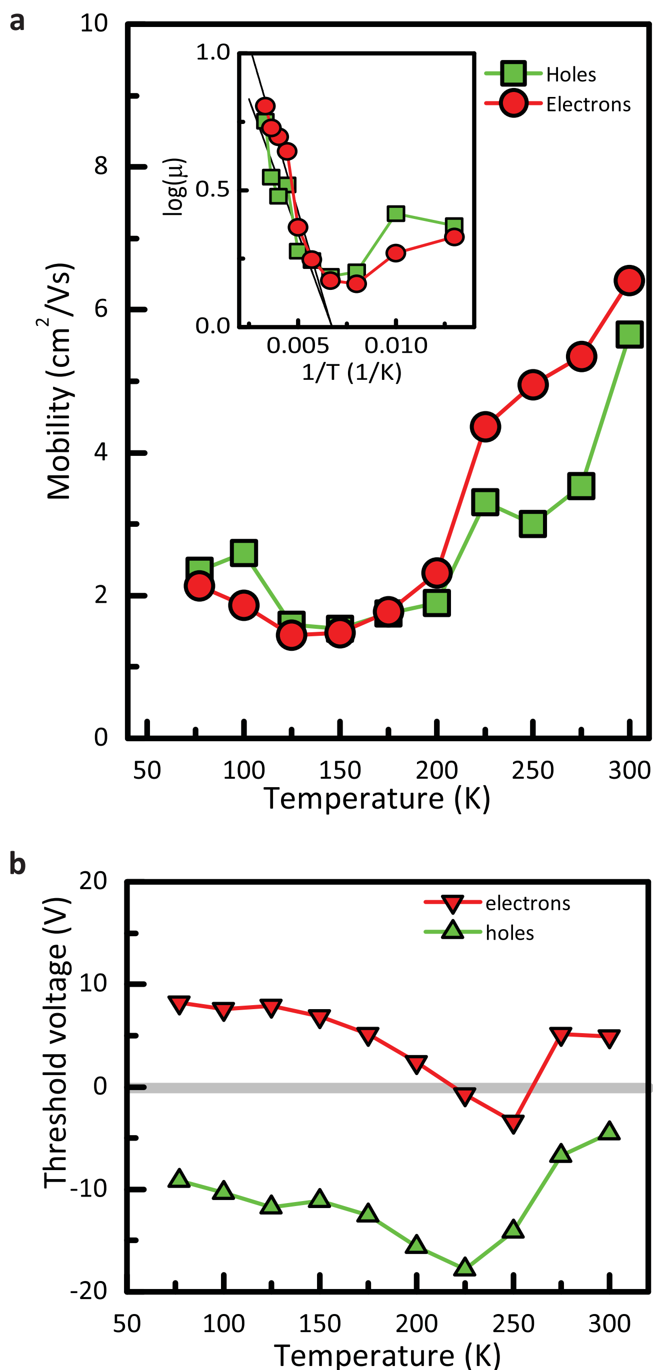

Figure 3. a) Temperature dependent intrinsic (contact resistance free) mobility values for holes (green squares) and electrons (red circles). (Inset) Logarithmic plot of the temperature-dependent carrier mobility, which fits an Arrhenius trend above 175 K. b) Temperature dependence of the threshold voltage values for hole and electron accumulation.

respectively. These anomalies in the mobility variation were only observed in FETs with preferred alignment of the tubes parallel to the channel length (see Figure S3, Supporting Information). The FETs with random network and orthogonal alignment to the channel length did not demonstrate such occurrence.

The behavior of the threshold voltage (V_{Th}) for holes and electrons accumulations in the ambipolar FET is shown in Figure 3b. The displayed threshold voltage values were extracted using the linear extrapolation of the transconductance (GMLE) method,[28,29] which are consistent with those obtained from Y-function method. At room temperature, the V_{Th} values are −4.5 V and 4.9 V for holes and electrons, respectively. The threshold voltage shifted toward negative values, the hole V_{Th} became −17.8 V at 225 K, and the electron V_{Th} to −3.4 V at 250 K. Lowering the temperature, further shifts back the threshold voltage values closer to the room temperature voltage. From 150 K down to 77 K, the holes V_{Th} remains at around −10.3 V and the electron V_{Th} at 7.5 V. The trend of the threshold voltage indicates that the density of electrons and holes do not significantly change with the temperature. Furthermore, the shift of the threshold voltage in the mid-temperature range happens simultaneously for holes and electrons. This might be attributed to the shift of the SWNT network Fermi level, instead of the variation of charge carrier trapping behavior either for holes or electrons. The shift of the Fermi level could be triggered by conformational changes and/or bonds shrinking of the polymer chains, which in the mid-temperature range may be substantial. Interestingly, from this mid temperature dip and going toward lower temperatures, a constant shift of the V_{Th} values toward the initial room temperature values is observed. Therefore, the anomalous behavior of the charge carrier mobilities is not the result of the change of accumulated carrier density.

Arrhenius plots of conductivity versus temperature (log σ *vs* T^{-1}) of holes and electrons at different applied V_G are shown in **Figure** 4a,b, respectively. In general, a linear relation of log σ versus T^{-1} suggests that the transport follows the nearest-neighbor-hopping (NNH) mechanism within the given temperature range. This appears to be valid only within the temperature range of 200–300 K. The hopping activation energy of holes decreases from 122.4 meV at V_G = −20 V to become 27.3 meV at V_G = −50 V. For electrons, the activation energy values are much smaller than for holes, 67.5 meV at V_G = 10 V which monotonously decrease to 27.5 meV at V_G = 50 V.

The obtained activation energy values are much smaller than what have been reported previously for the other semiconducting single-walled carbon nanotube networks. In particular, the hole activation energy is half of what has been reported by Gao and Loo[22] and it can be further reduced by the application of higher gate voltage. This indicates the high purity of our sample, which contains a high amount of semiconducting SWNT species and a minimum amount of residual polymer chains. It is also important to underline that this is the first report of the electron activation energy of SWNT networks, owing to the strong ambipolar behavior of our FETs.

At much lower temperature (<225 K, in Figure 4a,b), the conductivity trend deviated from the simple linear relation mentioned above. At low V_G, both hole and electron conductivity values reach a minimum and stabilize in a plateau. At V_G = −20 V, hole conductivity reaches the minimum value at around 225 K. At V_G = 10 V, the minimum of the electron conductivity is reached at 125 K. At higher V_G values ($|V_G| \geq 30$ V), both holes and electrons demonstrated anomalous increase of conductivity after passing the respective minima by further lowering the temperature. The hole conductivity increases then

© 2015 WILEY-VCH Verlag GmbH & Co. KGaA, Weinheim

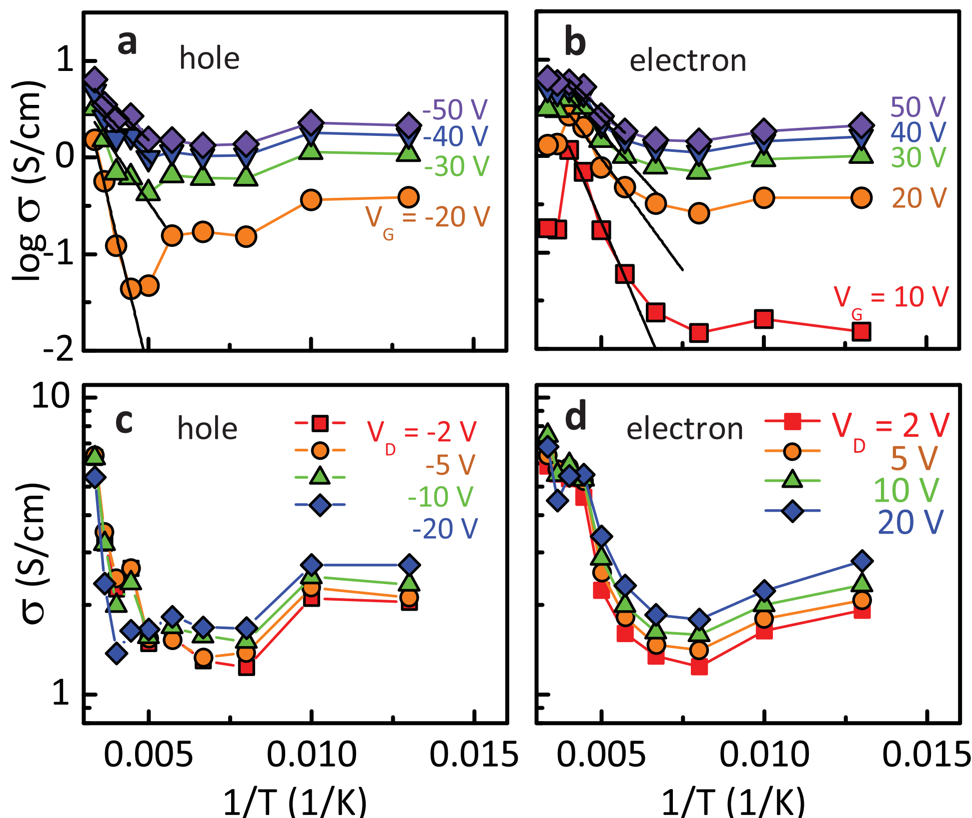

Figure 4. a) Temperature dependence of the holes, and b) electrons conductivity at fixed $V_D = -5$ V (for holes) and 5 V (for electrons) at different applied V_G. The conductivity values were extracted by assuming the thickness of the accumulation layer to be 5 nm, i.e., equivalent to the whole thickness of the nanotube network film. c) Temperature dependence conductivity of holes and d) electrons at fixed $V_G = 50$ V and different V_D.

reaches a plateau at temperature lower than 100 K. The increase of the conductivity is much more pronounced for holes than for electrons, and the increase persists until the temperature reached the lowest measurable temperature with our experimental apparatus (77 K). These conductivity anomalies strongly suggest that in semialigned nanotube network, the transport mechanism cannot be simply explained by hopping, either it is a simple thermally activated Arrhenius-type hopping, or a variable-range hopping.

The origin of this anomalous behavior of the electron and hole conductivity can be explained by the interplay between the percolation-type charge carrier transport in the nanotube network and the intrinsic charge carrier transport of the individual SWNTs. In this SWNT network, which was fabricated using an enriched semiconducting nanotube solution, the only remaining polymer chains are those wrapping the individual nanotubes.[12,13] In order to have charge carrier transported from one nanotube to another, holes or electrons should tunnel through the polymer chains that wrap the tubes. The intertube distance can be as small as 1 nm, but it is also determined by the conformation of the alkyl arms of the polymer acting as steric hindrance. While some of the alkyl arms are wrapping the nanotubes, some others, are perpendicular to the nanotube plane.[13] At low temperature, these standing alkyl arms could be prone to retract toward a hugging conformation[30,31] or to interlock with the alkyl chains from neighboring polymer wrapped nanotubes. Therefore, the intertube distance can become shorter. While the potential barrier for charge carrier hopping may remain unchanged, the intertube distance would make easier for the charge carrier to tunnel through the reduced barrier width. This is completely different from the fluctuation induced tunneling (FIT) model used for other nanotube networks,[22] in which the barrier width and height (due to the polymer) are considered to be constant in form of a parabolic energy barrier representation; thus cannot explain the increase of conductivity in the lower temperature regime.

It is known that a ballistic transport regime can be detected in carbon nanotubes. In this regime, the conductivity will increase by the decrease of temperature.[32] In our PF12-wrapped SWNT, the length of the nanotubes can be as long as 2.5 µm;[13] thus, it is possible that there are percolation path with a very limited number of nanotube-nanotube junctions (less than 10). Therefore, in semi-aligned pure sSWNT networks, the charge carrier transport at low temperature can be dominated by the intrinsic nature of few of the individual carbon nanotubes, masking the collective behavior that is dominant at higher temperature. FETs with shorter channel length show much earlier onset of mobility increase at low temperature (see Figure S5, Supporting Information). Nevertheless, we cannot completely ignore the possibility that the residual metallic species of the SWNTs may also become the origin of the conductivity increase. However, the optical absorption spectra (Figure 1d) of the SWNT solution indicates minimum signature of metallic species. Moreover, the FET devices exhibit high on–off ratio both at room temperature

© 2015 WILEY-VCH Verlag GmbH & Co. KGaA, Weinheim

(Figure 2a), and importantly, at low temperature. The high on/off ratio at low temperature is also mainly contributed by the low off-current of both holes and electrons, which is a strong proof that metallic tubes do not influence the transport properties of these devices.

The above observations make clear that polymer-wrapped semiconducting SWNT networks are complex hybrid material system. The properties of the network films are strongly determined not only the properties of the sSWNTs and the polymer used, but also the interaction between them. One of the nontrivial behaviors is, for example, the structural change of the polymer by temperature, due to the constriction of the nanotube as the consequence of wrapping. The peculiar feature observed here increase the interest toward the investigation of the temperature dependent transport behavior in the other ambipolar FETs based on polymer-wrapped SWNTs with different polymer backbones, different SWNT diameters, as well as different types of networks (random or aligned), including devices with record high on/off ratio of 10^8.[16] It would signify our understanding regarding the interweaving electronic properties between the SWNTs and the polymer species that wrapped them.

In conclusion, we reported temperature dependent transport measurements of ambipolar FETs using semialigned network of large diameter SWNT as active material. Anomalous temperature dependent nonlinear transport was observed for both holes and electrons. The nonlinear behavior deviates from both hopping transport and fluctuation induced tunneling mechanism. Furthermore, conductivity enhancement was observed at temperatures below 150 K. This behavior appears as determined by the intrinsic transport properties of the single tubes averaged by the network properties. The increase of the on/off ratio at low temperature makes us exclude for an effect determined by the few metallic tubes eventually present in the transistor channel.

Experimental Section

Preparation of Polymer-Wrapped Semiconducting SWNT Dispersion: Some details of the purification and separation of semiconducting SWNTs using poly(9,9-di-n-dodecylfluorene-2,-diyl) (PF12) has been explained in our previous reports.[13] PF12 were solubilized in toluene with concentration of 0.3 mg mL^{-1}. Similar weight of single-walled HiPCO nanotubes (Unidym, Sunnyvale, CA) was added into the polymer solution. The solution was then sonicated using a high power cup-horn sonicator, before it underwent a two-step ultracentrifugation to remove bundles, carbon contaminants, and metallic nanotubes. The first step was done at 40 000 rpm (190 000*g*) for 1 h. The formed pellet contained precipitated bundles was then removed. The upper part of supernatant containing the polymer-wrapped SWNT was again centrifuged at 55000 rpm (367 000*g*) for 5 h. The individualized SWNTs, which are pelletized by this process, were then redispersed in toluene. The purity of the SWNT solution was confirmed by the solution absorption spectra, which was acquired using UV/vis/NIR spectrophotometer (Shimadzu UV-3600) (see Section S7 of the Supporting Information for concentration determination).

Fabrication of Field-Effect Transistors with Semialigned SWNTs: The FET structures were fabricated on top of highly-doped Si wafer substrate with 230 nm thick thermally grown SiO_2, which is used as the gate dielectric of the device. To form a semi-aligned nanotube network, blade coating technique was performed using an automatic film applicator (Zehntner ZAA 2300, Switzerland). The deposition was performed with the substrate heated up to 55 °C. 20 µL of SWNT solution was dropped on the substrate and the flat blade moved above the substrate to spread the solution and remove its excess. To increase the nanotube density in the film, the process was repeated 10 times. Finally, the fabricated devices were heated at 140 °C for 3 h in the same glovebox where they were fabricated. The atomic force microscope (AFM, Bruker MultiMode 8), operated in tapping mode, was used to image the semi-aligned network.

Low Temperature Measurements of the Ambipolar FET: The FETs were measured using a low temperature probe station cryostat (Janis-ST500) equipped with 4 probe arms and a biased sample chuck, which are connected to Agilent E5270B Precision Measurement Mainframe. The ambipolar FETs were shortly exposed (<5 min) to the ambient conditions when they were transferred from the inert glovebox into the cryostat. The devices were pumped down in the cryostat, and annealed at 105 °C for 24 h in order to remove any adsorbates. After annealing, all FETs tested have restored their ambipolar characteristics. The samples were then cooled down by using liquid nitrogen, reaching the bottom (stable) temperature of 77 K. In addition to the drain current (I_D) and source current (I_S), the gate current (I_G) was also measured. The measured I_G values are always much lower than I_D and I_S, in general at least 1-order of magnitude lower of the off-current state.

Some experiments were also repeated in a cryogen-free refrigeration system (Pascal-OP101DE-12). These experiments were performed only down to 77 K to be consistent with the other measurements. The FET parameters were measured also using an Agilent E5270B Precision Measurement Mainframe.

Supporting Information

Supporting Information is available from the Wiley Online Library or from the author.

Acknowledgements

The authors would like to acknowledge P. Gordiichuk and Prof. A. Herrmann (University of Groningen) for the access to the atomic force microscope, as well as A. F. Kamp, R. Gooijaarts, J. Harkema for the technical support. Prof. Y. Iwasa (RIKEN-CEMS) is also acknowledged for the facility access to perform some additional measurements. The collaborative research program between the University of Groningen and Wuppertal University was made possible with financial support by Stichting voor de Technische Wetenschappen (STW, Utrecht, The Netherlands) and the Deutsche Forschungsgemeinschaft (DFG, Bonn, Germany).

Received: July 13, 2015
Revised: September 29, 2015
Published online: November 30, 2015

[1] L.-M. Peng, Z. Zhang, S. Wang, *Mater. Today* **2014**, *17*, 433.
[2] Z. Chen, D. Farmer, S. Xu, R. Gordon, P. Avouris, J. Appenzeller, *IEEE Electron Device Lett.* **2008**, *29*, 183.
[3] G. S. Tulevski, A. D. Franklin, D. Frank, J. M. Lobez, Q. Cao, H. Park, A. Afzali, S.-J. Han, J. B. Hannon, W. Haensch, *ACS Nano* **2014**, *8*, 8730.
[4] ITRS Working Groups, *International Technology Roadmap for Semiconductors 2013 Edition*, **2013**, ITRS Working Group.
[5] S. K. Samanta, M. Fritsch, U. Scherf, W. Gomulya, S. Z. Bisri, M. A. Loi, *Acc. Chem. Res.* **2014**, *47*, 2446.
[6] Y.-L. Zhao, J. F. Stoddart, *Acc. Chem. Res.* **2009**, *42*, 1161.
[7] A. D. Franklin, *Nature* **2013**, *498*, 443.

© 2015 WILEY-VCH Verlag GmbH & Co. KGaA, Weinheim

[8] C. Wang, K. Takei, T. Takahashi, A. Javey, *Chem. Soc. Rev.* **2013**, *42*, 2592.
[9] M. C. Hersam, *Nat. Nanotechnol.* **2008**, *3*, 387.
[10] H. Liu, D. Nishide, T. Tanaka, H. Kataura, *Nat. Commun.* **2011**, *2*, 309.
[11] A. Nish, J.-Y. Hwang, J. Doig, R. J. Nicholas, *Nat. Nanotechnol.* **2007**, *2*, 640.
[12] S. Z. Bisri, J. Gao, V. Derenskyi, W. Gomulya, I. Iezhokin, P. Gordiichuk, A. Herrmann, M. A. Loi, *Adv. Mater.* **2012**, *24*, 6147.
[13] W. Gomulya, G. D. Costanzo, E. J. F. de Carvalho, S. Z. Bisri, V. Derenskyi, M. Fritsch, N. Fröhlich, S. Allard, P. Gordiichuk, A. Herrmann, S. J. Marrink, M. C. dos Santos, U. Scherf, M. A. Loi, *Adv. Mater.* **2013**, *25*, 2948.
[14] R. Martel, T. Schmidt, H. R. Shea, T. Hertel, P. Avouris, *Appl. Phys. Lett.* **1998**, *73*, 2447.
[15] A. Javey, M. Shim, H. Dai, *Appl. Phys. Lett.* **2002**, *80*, 1064.
[16] V. Derenskyi, W. Gomulya, J. M. S. Rios, M. Fritsch, N. Fröhlich, S. Jung, S. Allard, S. Z. Bisri, P. Gordiichuk, A. Herrmann, U. Scherf, M. A. Loi, *Adv. Mater.* **2014**, *26*, 5969.
[17] T. Dürkop, S. A. Getty, E. Cobas, M. S. Fuhrer, *Nano Lett.* **2004**, *4*, 35.
[18] Y.-M. Lin, J. Appenzeller, J. Knoch, P. Avouris, *IEEE Trans. Nanotechnol.* **2005**, *4*, 481.
[19] K. Yanagi, H. Udoguchi, S. Sagitani, Y. Oshima, T. Takenobu, H. Kataura, T. Ishida, K. Matsuda, Y. Maniwa, *ACS Nano* **2010**, *4*, 4027.
[20] S. Luo, T. Liu, S. M. Benjamin, J. S. Brooks, *Langmuir* **2013**, *29*, 8694.
[21] T. Tanaka, K. Mori, E. Sano, B. Fugetsu, H. Yu, *Phys. E* **2012**, *44*, 997.
[22] J. Gao, Y.-L. (Lynn) Loo, *Adv. Funct. Mater.* **2015**, *25*, 105.
[23] S. Z. Bisri, C. Piliego, J. Gao, M. A. Loi, *Adv. Mater.* **2014**, *26*, 1176.
[24] H.-Y. Chang, W. Zhu, D. Akinwande, *Appl. Phys. Lett.* **2014**, *104*, 113504.
[25] I. Yagi, K. Tsukagoshi, Y. Aoyagi, *Appl. Phys. Lett.* **2005**, *86*, 103502.
[26] H. Sirringhaus, N. Tessler, R. H. Friend, *Science* **1998**, *280*, 1741.
[27] S. M. Sze, K. K. Ng, *Physics of Semiconductor Devices*, John Wiley & Sons, Hoboken, New Jersey, **2007**.
[28] S. Z. Bisri, E. Degoli, N. Spallanzani, G. Krishnan, B. J. Kooi, C. Ghica, M. Yarema, W. Heiss, O. Pulci, S. Ossicini, M. A. Loi, *Adv. Mater.* **2014**, *26*, 5639.
[29] M. Tsuno, M. Suga, M. Tanaka, K. Shibahara, M. Miura-Mattausch, M. Hirose, *IEEE Trans. Electron Devices* **1999**, *46*, 1429.
[30] S. Guha, J. D. Rice, Y. T. Yau, C. M. Martin, M. Chandrasekhar, H. R. Chandrasekhar, R. Guentner, P. Scanduicci de Freitas, U. Scherf, *Phys. Rev. B* **2003**, *67*, 125204.
[31] E. J. W. List, R. Guentner, P. Scanducci de Freitas, U. Scherf, *Adv. Mater.* **2002**, *14*, 374.
[32] A. Javey, J. Guo, Q. Wang, M. Lundstrom, H. Dai, *Nature* **2003**, *424*, 654.

© 2015 WILEY-VCH Verlag GmbH & Co. KGaA, Weinheim